

ORIGINAL ARTICLE

Nanoparticle-Mediated Cell Capture Enables Rapid Endothelialization of a Novel Bare Metal Stent

Brandon J. Tefft, PhD,¹ Susheil Uthamaraj, MS,² Adriana Harbuzariu, MD,¹ J. Jonathan Harburn, PhD,³ Tyra A. Witt, AAS, CVT,¹ Brant Newman, BS,² Peter J. Psaltis, MBBS, PhD,^{4,5} Ota Hlinomaz, MD, PhD,⁶ David R. Holmes, Jr., MD,¹ Rajiv Gulati, MD, PhD,¹ Robert D. Simari, MD,¹ Dan Dragomir-Daescu, PhD,⁷ and Gurpreet S. Sandhu, MD, PhD¹

Incomplete endothelialization of intracoronary stents has been associated with stent thrombosis and recurrent symptoms, whereas prolonged use of dual antiplatelet therapy increases bleeding-related adverse events. Facilitated endothelialization has the potential to improve clinical outcomes in patients who are unable to tolerate dual antiplatelet therapy. The objective of this study was to demonstrate the feasibility of magnetic cell capture to rapidly endothelialize intracoronary stents in a large animal model. A novel stent was developed from a magnetizable duplex stainless steel (2205 SS). Polylactic-co-glycolic acid and magnetite (Fe₃O₄) were used to synthesize biodegradable superparamagnetic iron oxide nanoparticles, and these were used to label autologous blood outgrowth endothelial cells. Magnetic 2205 SS and nonmagnetic 316L SS control stents were implanted in the coronary arteries of pigs ($n = 11$), followed by intracoronary delivery of magnetically labeled cells to 2205 SS stents. In this study, we show extensive endothelialization of magnetic 2205 SS stents (median 98.4% cell coverage) within 3 days, whereas the control 316L SS stents exhibited significantly less coverage (median 48.9% cell coverage, $p < 0.0001$). This demonstrates the ability of intracoronary delivery of magnetic nanoparticle labeled autologous endothelial cells to improve endothelialization of magnetized coronary stents within 3 days of implantation.

Keywords: magnetic stent, endothelialization, nanotechnology, cell-targeting

Introduction

INTRAVASCULAR STENT DEPLOYMENT creates a persistent prothrombotic milieu until endothelial cell coverage fully excludes the stent struts from contact with circulating platelets and the coagulation system. The process of endothelialization occurs over a period of several weeks and dual antiplatelet therapy is usually recommended for up to 12 months after the placement of a stent. Antiplatelet agents can place elderly patients and those with a bleeding diathesis at a higher risk of life-threatening bleeding and may be contraindicated in certain patients. In addition, recent clinical trials have presented conflicting recommendations for the duration of dual antiplatelet therapy with two European trials re-

commending <6 months^{1,2} and a larger FDA-sponsored US trial recommending at least 30 months.³ Rapid endothelialization of stent struts to reduce reliance on dual antiplatelet therapy may have a future role for patients with a history of stent thrombosis, or those at high risk for bleeding.

Attracting endothelial progenitor cells to the stent surface by using CD34 antibodies⁴ or capturing locally delivered cells⁵ has been proposed previously, and the emergence of nanotechnology has enabled newer modalities such as magnetic targeting.⁶⁻⁹ Early reports had validated the ability to magnetically capture living endothelial cells on stents and vascular grafts.¹⁰⁻¹² However, clinical translation proved difficult as existing vascular stents were nonmagnetizable, and most magnetizable metals were either nonbiocompatible

¹Department of Cardiovascular Medicine, Mayo Clinic, Rochester, Minnesota.

²Division of Engineering, Mayo Clinic, Rochester, Minnesota.

³School of Pharmacy & Institute of Cellular Medicine, Newcastle University, Newcastle-upon-Tyne, United Kingdom.

⁴Vascular Research Centre, South Australian Health and Medical Research Institute, Adelaide, Australia.

⁵School of Medicine, University of Adelaide, Adelaide, Australia.

⁶Department of Cardioangiopathy, St. Anne's University Hospital, Brno, Czech Republic.

⁷Department of Physiology and Biomedical Engineering, Mayo Clinic, Rochester, Minnesota.

or lacked the mechanical properties considered critical for a stent.

We recently developed a novel duplex stainless steel bare metal stent that can be magnetically functionalized for nanotechnology-based applications, including the capture of appropriately labeled endothelial cells.^{13,14} Medical grade polylactic-co-glycolic acid (PLGA) and magnetite (Fe_3O_4) were used to develop biodegradable superparamagnetic iron oxide nanoparticles (SPIONs) for magnetic cell labeling, and these underwent extensive evaluation to define optimal biocompatibility.¹⁵ An analysis of the results of magnetized duplex stainless steel stent implantation and SPION-mediated endothelialization in an *in vivo* animal model are presented in this study.

Materials and Methods

Study design

The objective of this research was to demonstrate rapid healing of magnetically endothelialized stents at 3 days and biocompatibility of magnetically endothelialized stents at 30 days. To assess these outcomes, we placed nonmagnetic control stents and magnetically endothelialized stents into the coronary arteries of healthy, female pigs. The 3-day samples were analyzed for strut area coverage as a primary measure of stent healing. These samples were also scored for quality of strut coverage (bare strut, thin fibrous tissue, or thicker neointimal tissue) as a secondary measure of stent healing. The 30-day samples were analyzed histologically by a pathologist for biocompatibility.

Precedent data were not available for a power calculation, so a sample size of 10 pigs was selected for each time point based on the rule of 12 for pilot studies,¹⁶ our previous experience, and a desire to use animals conservatively. Samples from pigs that did not survive to the designed study endpoint and samples that were damaged during processing were excluded from the final healing analysis. Outliers were not determined or excluded. Randomization of stent placement was not possible because placing the nonmagnetic stent proximally to the magnetic stents allowed for concentrated cell delivery to the magnetic stents only.

Cell culture

Autologous porcine blood outgrowth endothelial cells (BOECs) were isolated from 50 to 200 mL of peripheral blood using density gradient centrifugation (No. 17-1440, Ficoll-Paque Plus; GE Healthcare Life Sciences, Piscataway, NJ) as previously described.¹⁷ The cells were cultured on fibronectin-coated flasks (No. 33016-015; Gibco, Waltham, MA) using EGM-2 medium (No. CC-3162; Lonza, Basel, Switzerland) supplemented with 10% fetal bovine serum (No. F-0500-A; Atlas Biologicals, Fort Collins, CO) at 37°C in the presence of 5% CO_2 . Highly proliferative BOECs were obtained after 2 weeks in culture. These cells were passaged upon reaching 80% confluence, and the first two passages were used for studies.

PLGA-magnetite SPION synthesis and cell labeling

PLGA-magnetite SPIONs (120 nm diameter) were synthesized by coating PLGA (PURASORB® PDLG 7502, 75:25 lactide:glycolide; Purac, Amsterdam, The Netherlands)

onto 10 nm diameter magnetite cores as previously described.^{15,18,19} Three variants of PLGA-magnetite containing 40, 80, and 120 mg/mL magnetite were tested *in vitro*, and preliminary analysis indicated that the PLGA-magnetite containing the lowest concentration of iron (40 mg/mL magnetite) was adequate for magnetic cell capture. Cells were incubated with 200 μg of SPIONs per mL of culture medium at 37°C for 16 h, washed with phosphate-buffered saline, treated with 0.25% trypsin/EDTA, and used for experiments. This SPION concentration has been shown to be safe for endothelial cells^{20,21} and endothelial progenitor cells.²² For some experiments, cells were also labeled with a red carbocyanine membrane fluorescent tag (CM-DiI, No. V-22888; Life Technologies, Waltham, MA) for 30 min at 37°C.

Confirmation of cell labeling with endocytosed iron

BOECs were incubated for 16 h with optimal SPION concentrations and stained with Prussian Blue (Sigma-Aldrich, St. Louis, MO) to visualize endocytosed iron and Nuclear Fast Red solution (Sigma-Aldrich) to delineate the nuclei, following which the cells were imaged using light microscopy. Cells were also treated with Trump's fixative and embedded in plastic resin, following which transmission electron microscopy was used to confirm the intracellular location of iron particles.

Development of magnetic vascular stents

A survey of metals approved for medical implantation yielded no magnetizable materials. A variety of magnetizable metals, including cobalt chromium and stainless steel alloys (304, 108, 430FR, CCM, 465, L605, and 2205), were identified with assistance from metallurgy and magnetics experts. The 2205 duplex stainless steel (2205 SS) was selected due to its favorable mechanical properties, corrosion resistance, weak ferromagnetic properties, and similarity to clinically utilized 316L stainless steel (316L SS).

An independent materials testing laboratory (Toxikon Corp, Bedford, MA) was contracted to test the biological toxicity of the 2205 SS material based on ISO 10993 standards. Eight tests were selected to evaluate cytotoxicity (L929 MEM Elution and Neutral Red Cytotoxicity Test), irritation (Intracutaneous Injection), acute systemic toxicity (Acute Systemic Injection and Material Mediated Rabbit Pyrogen Test), and hemocompatibility (Hemolysis Complete, *In vitro* Hemocompatibility Assay, and Unactivated Partial Thromboplastin Time).

2205 SS stents were fabricated by drilling tube stock and laser cutting the strut pattern. Stents used in the 3-day pig implantation study were 3.0 \times 15 mm, featured a hinge point design to reduce the risk of strut fracture,^{13,14} and were crimped onto balloons using a commercial crimping tool (No. RMC-M1; Blockwise Engineering, Tempe, AZ) to facilitate more uniform expansion. Stents used in the 30-day pig implantation study were 3.0 \times 18 mm. All stents were electropolished and chemically annealed to improve surface characteristics. The 3-day pig study necessitated the fabrication of identical 316L SS stents to serve as nonmagnetic controls.

Magnetization and *in vitro* cell capture of 2205 SS stents

Stents were magnetized using a 1 min contact with a 1.0 T rare earth magnet (No. D1000P; Amazing Magnets,

Anaheim, CA) oriented to allow the magnetic field to cross at 90° to the long axis of the stent. Standard fluorescence microscopy was used to visualize attachment of CM-DiI-stained BOECs on the surface of 2205 SS stents as well as 316L SS control stents. Video recording of cell capture provided additional confirmation of ongoing cellular attraction.

In vivo cell attraction to magnetic stents

All animal studies were approved by the Institutional Animal Care and Use Committee at Mayo Clinic. Female Yorkshire Cross domestic pigs weighing 40–50 kg (4–5 months old) were used for coronary stent implantation and autologous cell delivery. The pigs were studied for 3 days ($n = 11$) or 30 days ($n = 10$). Before the procedure, pigs were anesthetized using an intramuscular injection of 2–3 mg/kg xylazine, 5 mg/kg tiletamine/zolazepam, and 0.05 mg/kg atropine followed by intubation and continuous inhalation of 1.2–1.5% isoflurane to maintain anesthesia during the procedure. Body temperature was monitored and maintained with warm blankets. A carotid cutdown was performed to allow for sheath placement and transcarotid access. The right coronary artery was selectively cannulated using a 7–8 F Judkins JL3.5 coronary guide catheter. Stents were sterilized by autoclaving and then magnetized by contact with a rare earth magnet enclosed within a sterile plastic bag. Stents were implanted in each animal using an appropriately selected 3.0 × 20 mm or 3.5 × 20 mm balloon inflated to achieve a stent-to-artery ratio of 1.1-to-1.0. The animals received daily 75 mg clopidogrel and 325 mg aspirin starting 3 days before stent placement and continuing until stent harvest. Unfractionated heparin (100–200 units/kg bolus) was used during the procedure to maintain an activated clot time of 250–350 s.

The 3-day studies used magnetized 2205 SS stents and identically fabricated nonmagnetizable 316L SS stents as controls. The use of nonmagnetizable 316L SS controls enabled the use of two additional magnets external to the chest wall to further enhance the magnetic field strength induced within the implanted 2205 SS magnetic stents. Two 1.0 T permanent magnets were strapped anterior and right lateral to the chest wall of the pig. This was done immediately before delivery of $\sim 2.0 \times 10^6$ autologous BOECs labeled with PLGA-magnetite SPIONs and CM-DiI and maintained for up to 2 h afterward. Cells were delivered at the site of the 2205 SS stents during a 2 min flow occlusion using an over the wire balloon catheter inflated proximally to the stents. Flow was restored after allowing an additional 2 min contact period between the cells and the stents. The control 316L SS nonmagnetic stents were not directly exposed to delivered BOECs. The vessels were harvested after 3 days, and the stented segments were sectioned longitudinally into two halves to evaluate surface coverage. One half was examined under light and fluorescence microscopy, while the other half was subjected to scanning electron microscopy (SEM) to quantify surface endothelial coverage. Selected samples were stained with Hoechst nuclear stain and CD31 antibody (No. NB100-65336; Novus Biologicals, Littleton, CO) or mouse IgG isotype control antibody (No. MAB002; R&D Systems, Minneapolis, MN) before fluorescence microscopy.

The 30-day studies used magnetized 2205 SS stents with identical nonmagnetized (degaussed) 2205 SS stents for

controls. Approximately 2.0×10^6 autologous BOECs labeled with PLGA-magnetite SPIONs were delivered at the site of the 2205 SS stents as in the 3-day study. After 30 days, the coronary artery segments were carefully isolated and immersed in 10% formalin. Stented arteries were then embedded in plastic, sectioned, and stained by hematoxylin and eosin, Movat's Pentachrome, and Mallory's Prussian Blue (for iron). The slides were examined and scored by a pathologist, and key features, including neointima thickness, were measured.

Assessment of endothelialization at 3 days

A quantitative and a qualitative analysis were performed on all segments of SEM visualized stent struts. Images used for analysis were magnified 25× such that the entire height of the longitudinally sectioned vessel could be visualized. Several images were taken along the length of each vessel such that each half stent ring was visualized and analyzed in its entirety. Therefore, the entire strut area of the half of the vessel designated for SEM imaging was analyzed for cell coverage.

Quantitative analysis was done by measuring the endoluminal strut area covered with cells versus the total endoluminal strut area of each stent. Anything other than a bare strut was considered covered to minimize operator bias and subjectivity. Two independent operators used an area marking tool in image analysis software (Photoshop CS6; Adobe, San Jose, CA) to measure the areas and the measurements were averaged.

Qualitative strut coverage was assessed by seven blinded observers and averaged. The following definitions were provided for scoring: 0 = little to no coverage, 1 = partial coverage with a thin fibrous tissue, 2 = patchy coverage with a mixture of thin fibrous tissue and thicker neointima, and 3 = near complete or complete coverage with thicker neointima.

Statistical analysis

A general linear model was used to determine treatment effect on stent cell coverage (JMP v10.0.0; SAS Institute, Cary, NC). The correlation between multiple observations from the same pig was modeled using a random effect for pig. A logit transformation was used on coverage proportion. Proportions equal to 1.000 were converted to 0.995 for purposes of the logit transformation. An *F* test was used on the estimate of treatment effect to calculate a two-sided *p*-value. A *t* test was used to compare differences between groups for measured features in the 30-day study. A *p*-value of <0.05 was considered statistically significant. Data with asymmetrical distributions are presented as median and interquartile range (IQR).

Results

Confirmation of SPION incorporation

Prussian Blue staining of cells incubated with 200 µg/mL of PLGA-magnetite SPIONs confirmed the presence of iron particles in the majority of cells (Fig. 1A). Transmission electron microscopy images verified the presence of endocytosed particles within cytoplasmic endosomes (Fig. 1B). The particles are observed to be in distinct clusters and definitively incorporated within the cell membrane.

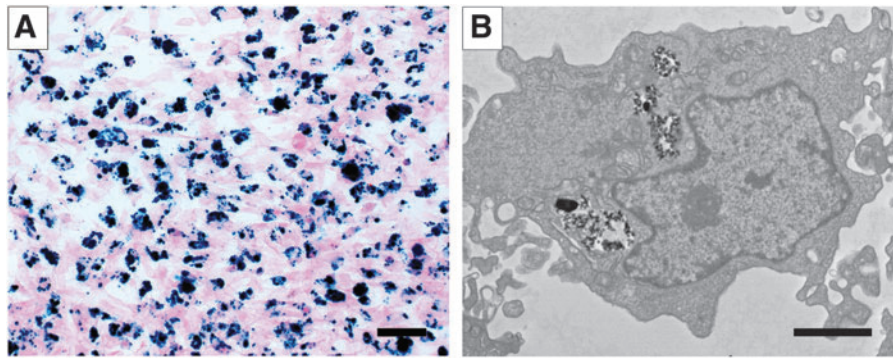


FIG. 1. Cellular uptake of magnetic nanoparticles. (A) Prussian Blue staining of BOECs labeled with PLGA-magnetite SPIONs showing nuclei (*pink*) and iron particles (*blue*). (B) Transmission electron microscopy image of BOEC labeled with PLGA-magnetite SPIONs. Scale bars are (A) 50 μm and (B) 2 μm . BOECs, blood outgrowth endothelial cells; PLGA, polylactic-co-glycolic acid; SPIONs, superparamagnetic iron oxide nanoparticles.

Biological toxicity of 2205 SS

The 2205 SS material did not demonstrate any biological toxicity effects when evaluated using selected tests from the ISO 10993 standard. The cytotoxicity tests indicated that 2205 SS was not considered to have a cytotoxic effect. The irritation test indicated that 2205 SS did not show a significantly greater biological reaction than the control articles. The acute systemic toxicity tests indicated that 2205 SS did not induce a significantly greater biological reaction than the control extracts and was considered nonpyrogenic. Finally, the hemocompatibility tests indicated that 2205 SS was considered nonhemolytic, was considered having no effect on selected hematological parameters, and was considered having no effect on coagulation of human plasma. Summaries of the individual biological toxicity tests are available in the Supplementary Data (Supplementary Data are available online at www.liebertpub.com/tea).

Magnetization of 2205 SS stents and confirmation of cell capture

Fluorescence microscopy was used to visualize attachment of CM-DiI and PLGA-magnetite SPION-labeled endothelial cells on the surface of 2205 SS and 316L SS control stents (Fig. 2). Video recording of cell capture using fluorescence microscopy provided additional confirmation of ongoing cellular attraction (Supplementary Video SV1).

In vivo 3-day stent study

A 3-day study was carried out using one proximally placed 316L SS stent and two distally placed magnetized 2205 SS stents in the right coronary artery (Fig. 3). Externally placed magnets were used to induce stronger magnetization within the stents, and these were left in place

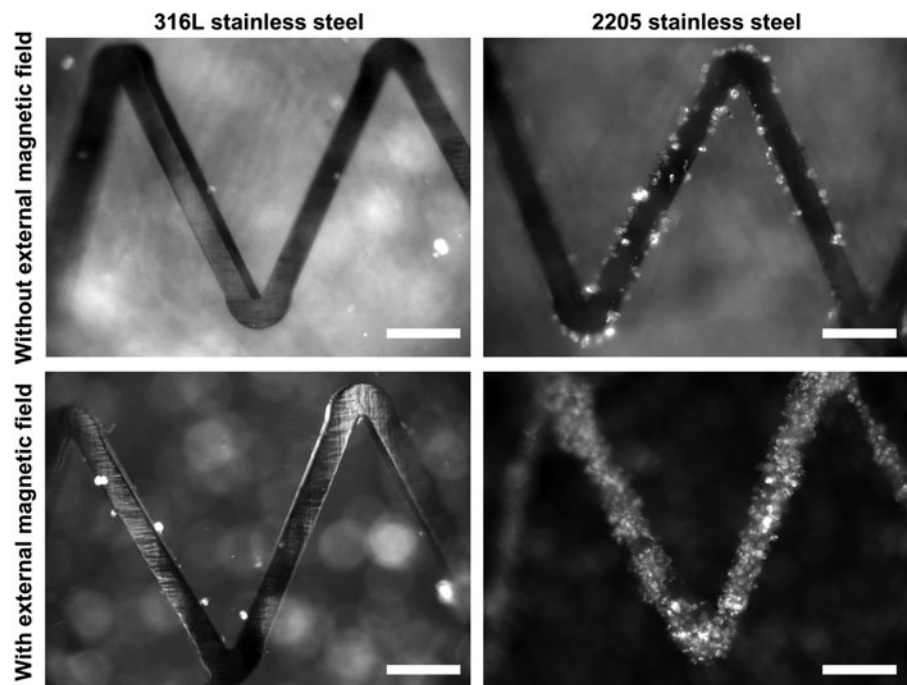


FIG. 2. *In vitro* cell capture study. PLGA-magnetite SPION-labeled BOEC capture on 316L SS and 2205 SS stents. 2205 SS (magnetic) stents exhibit superior cell capture compared with 316L SS (nonmagnetic) stents and the presence of an external magnetic field results in a more uniform and enhanced cell capture on the 2205 SS stents. Scale bars are 300 μm .

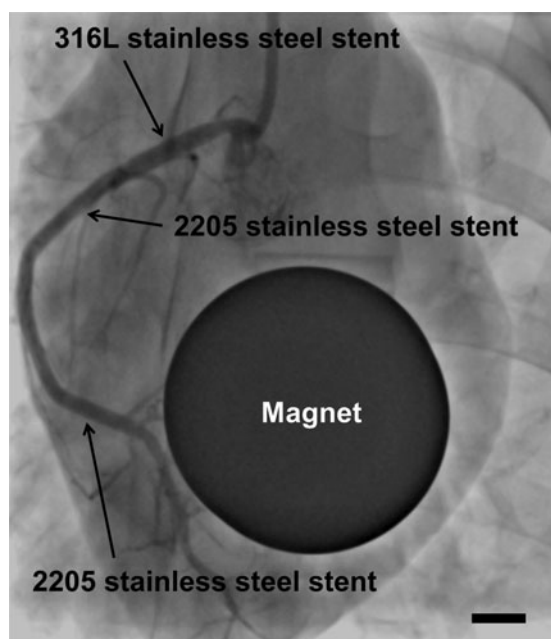


FIG. 3. Three-day pig study procedure. Angiogram of pig chest following stent implantation into the right coronary artery. Arrows indicate stent locations. The stents are difficult to discern due to the presence of intravascular contrast agent. Dark circular object is a rare earth magnet placed anterior to the chest. An identical magnet (not in image) was also present on the right lateral side of the thorax. Scale bar is 1 cm.

for up to 2 h following the delivery of labeled cells. Stents were analyzed at 3 days.

All pigs except one survived to the designed study end point of 3 days. One pig died of ventricular fibrillation immediately following placement of the 2205 SS stents and before placement of the 316L SS stent and cell delivery. While we cannot rule out the possibility that the novel stent material caused the arrhythmia, it is more likely explained by the general sensitivity of pigs to coronary interventions. This pig was excluded from further analysis.

All 18 2205 SS stents and all 9 316L SS stents were widely patent upon gross visual analysis at explant. One 316L SS

control stent sample, which was observed to have poor healing (i.e., a very thin and fragile neointima with poor integration into the vessel wall), was damaged during processing and excluded from further analysis. Thus, $n=18$ 2205 SS stents and $n=8$ 316L SS stents were analyzed from $n=9$ pigs. After the conclusion of the 3-day study with $n=10$ pigs, one additional pig ($n=1$) was used for separate immunohistochemistry analysis.

Light microscopy showed glistening 316L SS struts that appeared to have little tissue coverage, whereas the 2205 SS struts were almost fully covered beneath a layer of tissue (Fig. 4). Fluorescence microscopy showed excellent capture of delivered cells along the struts of the 2205 SS stents (Fig. 4). SEM analysis of each stent validated this observation (Fig. 4). The 2205 SS stents had homogenous tissue coverage consistent with that expected of endothelium, whereas the 316L SS stents had patchy coverage of an indeterminate origin that likely represented a mix of inflammatory cells, endothelium, and resolving thrombus. Uniformly strong cell membrane staining with a CD31 antibody confirmed the endothelial cell phenotype of delivered (colocalized with CM-DiI) and native (noncolocalized with CM-DiI) cells on the luminal surface of stented vessels (Fig. 5). Quantitative analysis of strut area covered with cells versus the total strut area showed statistically significant improvement with magnetic 2205 SS stents (median 98.4%, IQR 94.0–100.0%) compared with the nonmagnetic control 316L SS stents (median 48.9%, IQR 23.5–65.9%, $F=174.2$, $p<0.0001$) (Fig. 6A). Qualitative coverage was assessed by seven blinded observers, and this validated the presence of higher quality coverage for the magnetic 2205 SS stents ($F=63.4$, $p<0.0001$) (Fig. 6B).

In vivo 30-day stent study

All 10 pigs survived to the designed study end point of 30 days. These pigs appeared clinically healthy as indicated by alertness and activity. No signs of distress, pain, anorexia, withdrawal, dehydration, or general malaise were noted. The explanted hearts did not show signs of infarct on the exterior myocardium.

All the 10 magnetized 2205 SS and all the 10 nonmagnetized 2205 SS stents were widely patent upon gross visual analysis at explant. Four stents from the first two

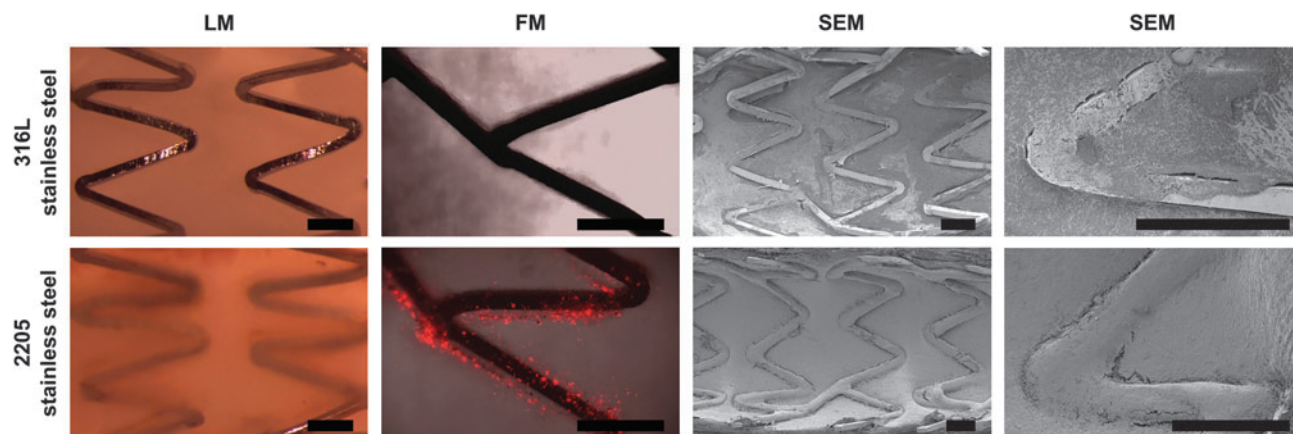


FIG. 4. Three-day pig study explants. Microscopy images of pig arteries stented with 316L SS and 2205 SS stents for 3 days. Scale bars are 500 μm . FM, fluorescence microscopy; LM, light microscopy; SEM, scanning electron microscopy.

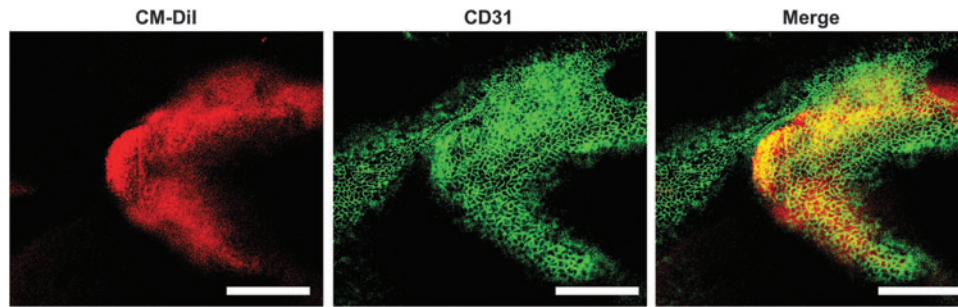


FIG. 5. Endothelial cell phenotyping. Fluorescence microscopy images of pig arteries stented with 2205 SS stents for 3 days. Cells are labeled for delivered cells (red) and CD31 (green). Colocalization of red and green signal (i.e., yellow signal) indicates delivered endothelial cells whereas green signal alone indicates endogenous endothelial cells. Scale bars are 200 μm .

animals were excluded from histologic analysis due to sub-optimal processing. Histologic analysis was performed on cross sections cut through the proximal, mid, and distal ends of eight magnetized and eight nonmagnetized stents. Mild to moderate neointimal proliferation was noted in all stents (Fig. 7). Iron staining confirmed traces of residual iron from the cells captured adjacent to the magnetized 2205 SS stent struts. There was no unexpected inflammation, corrosion, nor vascular injury attributable to the novel 2205 SS stents. Qualitatively, the magnetized stents appeared to have better-organized neointimal and endothelial layers. Quantitative analysis did not yield any differences in the healing of the nonmagnetized and magnetized stents as all stents had healed fully by 30 days. When neointimal thickness was normalized to wall thickness, the magnetized stents had only an 8.3% thinner neointima when compared with nonmagnetized stents (0.44 ± 0.19 vs. 0.48 ± 0.19), which was not a statistically significant difference ($p = 0.11$).

Discussion

The ability to rapidly endothelialize implanted intravascular devices can lead to substantial improvements in the quality and safety of these procedures. Our previously reported proof of concept studies utilized 10 μm nickel-plated clinical stents,¹⁰ but nickel is nonbiocompatible and often allergenic. Duplex stainless steels such as 2205 SS are weakly magnetizable, and exposure to an external magnetic field enhances their ability to attract iron-based particles. As demonstrated by the results, implantation of magnetized 2205 SS stents followed by delivery of PLGA-magnetite

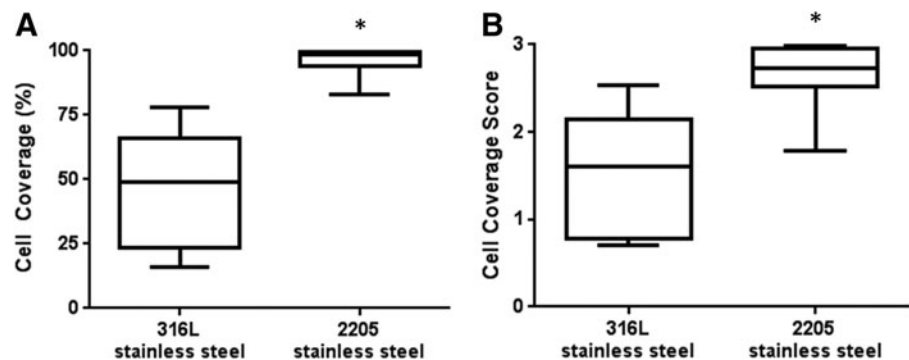
SPION-labeled autologous endothelial cells led to a significant improvement of endothelialization at 3 days.

BOECs are a homogenous, distinctly endothelial population of cells derived from nonphagocytic precursors.^{17,23,24} These cells have been shown to be purely endothelial in phenotype and function (morphology, expression of endothelial but not monocytic surface antigens, and expression of endothelial specific proteins) in multiple human and animal models.^{25,26} This is in contrast to “endothelial progenitor cells,” a different population of cells, which do express high degrees of phagocytic markers.

The ability to capture SPION-labeled BOECs on the surface of magnetized nickel-plated bare metal stents was first reported in a large animal model in 2006.¹⁰ Subsequent progress required developing a new generation of stent that was magnetizable and biocompatible. The search for candidate magnetic materials initially revealed several soft steels with limited structural properties and numerous non-biocompatible rare earth derivatives. The duplex stainless steels such as 2205 SS are structurally very similar to, but stronger than, clinical grade 316L SS and are often used for construction in corrosive marine environments. Duplex stainless steels also have an ability to retain a weak magnetic field, thereby making them an attractive option for transient magnetic “functionalization” to capture appropriately labeled therapeutic agents.

Stent design must allow for large-scale plastic deformation during crimping onto a balloon followed by another large-scale plastic deformation during deployment, and the surface finish must be consistently free of defects. Finite element analysis, laser cutting, electropolishing, and chemical

FIG. 6. Cell coverage analysis. Cell coverage of 316L SS ($n = 8$) and 2205 SS ($n = 18$) stents after 3 days of implantation into pig coronary arteries. (A) Percentage of stent strut surface covered by cells. (B) Scoring of neointima coverage from 0 (bare strut) to 3 (fully covered strut). * $p < 0.0001$. Data shown as median and IQR. IQR, interquartile range.



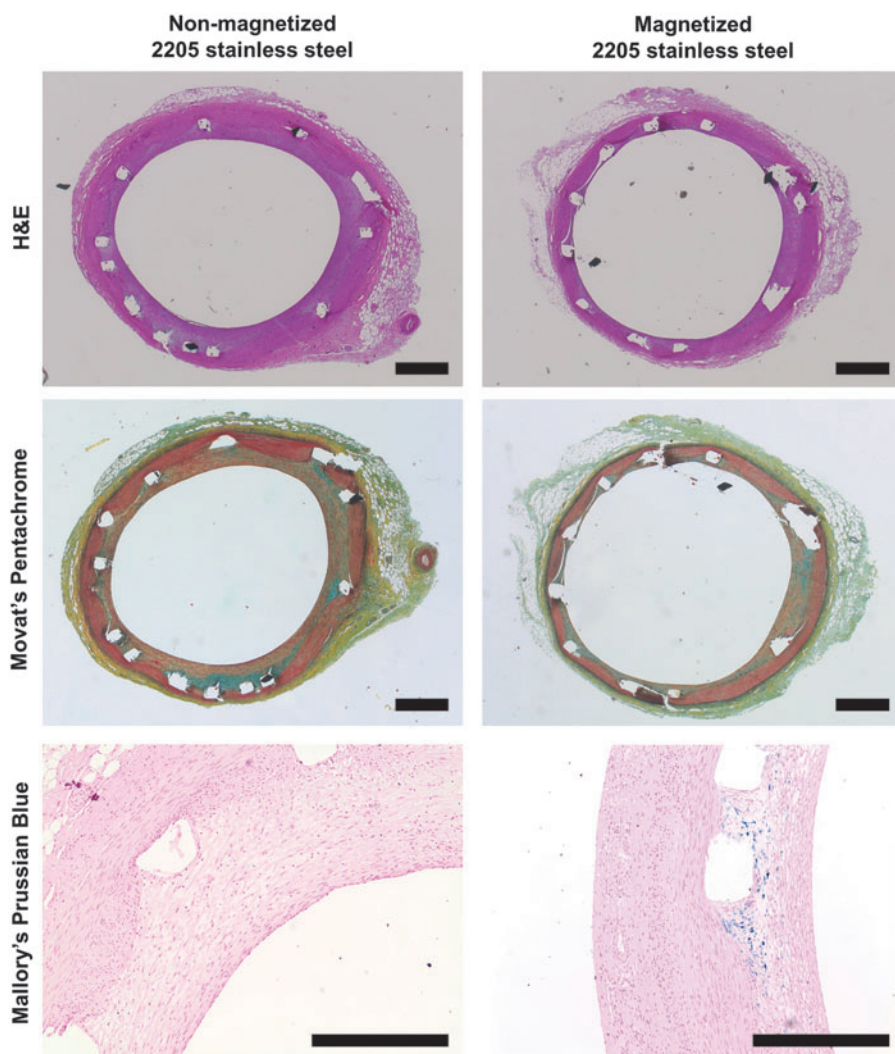


FIG. 7. Thirty-day pig study explants. Histology of pig arteries stented with 2205 SS stents for 30 days. The slides are stained with H&E (nuclei appear *blue* and cytoplasm appears *pink*), Movat's Pentachrome (elastin appears *black*, collagen appears *yellow*, fibrin appears *bright red*, and muscle appears *red*), and Mallory's Prussian Blue (iron appears *blue*, nuclei appear *red*, and background appears *pink*) as indicated. With the Mallory's Prussian Blue stain, iron-loaded cell capture is evident in the vicinity of magnetic stent struts. Scale bars are 300 μ m. H&E, hematoxylin and eosin.

annealing techniques were utilized to optimize the manufacture of 2205 SS and 316L SS stents.^{13,14} Geometrically identical 316L SS stents were manufactured to enable a direct comparison between a traditional bare metal stent and a cell-capturing magnetizable duplex stainless steel bare metal stent.

Biodegradable PLGA-magnetite SPIONs provided an effective and safe means for cell labeling at lower levels of iron loading.²⁷ PLGA is an FDA-approved polymer and has been used for over 30 years for intracellular drug delivery.²⁸⁻³¹ *In vivo* degradation is well documented and can be controlled by molecular weight, crystallinity, ratio of lactide:glycolide, and nanoparticle size.³²⁻³⁴ To ensure good manufacturing practice grade PLGA and well characterized *in vivo* biodegradation profile, the industry standard PURASORB PDLG 7502 was used to create the PLGA-coated SPIONs (120 nm diameter), and these were synthesized using an oil-in-water emulsion-diffusion method as described previously.¹⁵ The *in vivo* use of magnetite nanoparticles and subsequent clearance and biodegradation is well documented with the use of ferumoxides and dextran-coated small particles of iron oxides, used clinically to identify tumors of the liver and treatment of iron deficiency anemia in adult patients with chronic kidney disease.³⁵⁻³⁷ An important characteristic of ultrasmall particles of iron oxides in general is that they are biodegradable within cells, with the iron entering the systemic iron pool of

the individual.³⁸ PLGA-coated SPIONs have been used to magnetically label a large number of cell types for *in vivo* noninvasive cell tracking with no detectable cytotoxicity.^{39,40} A recent study showed 80% *in vivo* biodegradation of mesenchymal or neural stem cell-labeled PLGA-coated SPIONs (75:25, 105 nm, 83.7 weight percent magnetite) over 12 weeks.⁴¹ These particles had significantly higher internal concentrations of iron and similar overall particle size to the PLGA-coated SPIONs used within our study.

The efficacy of cell capture can be enhanced by increasing the concentration of magnetic particles within the cells. This may be achieved by utilizing a less cytotoxic SPION formulation that can be administered at a higher concentration⁴² as higher doses of iron appear to be more cytotoxic.^{43,44} The efficacy of cell capture can also be enhanced by increasing the strength of the magnetic force applied to the particles. This may be achieved by utilizing a more strongly ferromagnetic material, by changing the stent strut pattern to create stronger or additional magnetic poles, or by applying an external magnetic field during cell capture.^{6,45} The external magnetic field concept works by producing a stronger magnetic field and higher local field gradients, both of which are directly proportional to magnetic force,⁴⁶ and has previously proven effective for cell capture^{11,47,48} and drug targeting.⁴⁹⁻⁵² Bench testing confirmed that the concept of enhanced cell

capture by placing two external magnets at a 20–30 cm distance would work for 2205 SS stents. This was translated to the 3-day animal study by placing two magnets adjacent to the chest of the pig.

As seen in the results, healing at 3 days was markedly enhanced in the magnetized 2205 SS stents. Red fluorescent CM-DiI labeled cells are clearly seen lining the struts and light microscopy confirms excellent strut coverage compared to the glistening uncovered surface visible on the nonmagnetic 316L SS struts. The SEM images show statistically significant improvement in endothelialization, with qualitative improvement in coverage quality reported by independent observers. CD31⁺ endothelial cell antigen expressed by BOECs is seen in the cells covering the strut. The red CM-DiI cell surface marker is also seen colocalizing over the stent strut, thereby confirming the presence of delivered BOECs. As seen qualitatively in Figure 4, the tissue lining the control stents was patchy and, while not characterized in this study, likely consisted of a mix of inflammatory cells, platelets, and some endothelial cells. However, the fragility of this early tissue made immunohistochemistry exceedingly difficult. We elected to take a conservative approach toward coverage analysis of the control stent and included any significant coverage in the “covered” category yielding a 49% median coverage for the control stents.

The 30-day studies with the magnetized and nonmagnetized 2205 SS stents had a primary objective of assessing tissue effects due to the new implantable metal and were notable for a lack of any unusual inflammation or stent thrombosis during this period. We qualitatively observed scattered chronic inflammation in the 30-day studies as has previously been described in the porcine model of stenting, with predominantly smooth muscle cells and occasional chronic inflammatory cells present.⁵³ The presence of inflammatory cells adjacent to stent struts is also a well-established phenomenon in human coronaries, with chronic inflammation commonly observed adjacent to the stent struts beyond 12 days.⁵⁴ These observations are consistent with the lack of biological toxicity demonstrated for 2205 SS when subjected to selected tests based on the ISO 10993 standard.

These pilot studies were performed within normal vessels in pigs, and the applicability of this approach for treating diseased coronary arteries in an elderly human population is currently unknown. Hematologic disorders and other comorbidities may also impact the quality and availability of autologous BOECs, and the requirement to culture cells limits potential application to planned procedures only. Human safety studies shall be required to validate the novel stent material and SPIONs. The long-term vascular effects of low-level exposure to magnetism remain unknown.

Our study was designed to compare the current standard of care (i.e., 316L SS stents without cell delivery) to our novel magnetic endothelialization approach. Consequently, we did not study healing of the 2205 SS stents without cell delivery and it remains unknown if weak ferromagnetism alone can induce rapid stent healing. Furthermore, the use of a healthy pig model resulted in similar healing of all stents by 30 days, and it is possible that improved healing of magnetically endothelialized stents may be observed in a disease model that better represents clinical populations.

This is the first report of magnetically directed endothelial cell coverage of an implanted coronary stent in a large an-

imal model. The ability to magnetically guide living cells and other therapeutic agents to a specific site within the body opens up the possibility for developing novel treatment options for a variety of medical disciplines. Adaptations of this strategy could be used to deliver a cell-based therapeutic effect for regenerating tissues, and also conceivable is the ability to deliver an oncolytic effect for treating malignant tumors.

Acknowledgments

The authors gratefully acknowledge Dragan Jevremovic, MD, PhD, for pathological analysis of histology slides and Ryan Lennon for assistance with study design and statistical analysis. Funding provided by European Regional Development Fund—FNUSA-ICRC (No. CZ.1.05/1.1.00/02.0123), American Heart Association Scientist Development Grant (AHA No. 06-35185N), and National Institutes of Health (T32 HL007111, K99 HL129068).

Disclosure Statement

Mayo Clinic owns patents and intellectual property filings related to this work with D.R.H., R.G., R.D.S., D.D.-D., and G.S.S. listed as inventors. No competing financial interests exist for B.J.T., S.U., A.H., J.J.H., T.A.W., B.N., P.J.P., and O.H.

References

- Gilard, M., Barragan, P., Noryani, A.A., *et al.* 6- Versus 24-month dual antiplatelet therapy after implantation of drug-eluting stents in patients nonresistant to aspirin: the randomized, multicenter ITALIC trial. *J Am Coll Cardiol* **65**, 777, 2015.
- Colombo, A., Chieffo, A., Frasher, A., *et al.* Second-generation drug-eluting stent implantation followed by 6-versus 12-month dual antiplatelet therapy: the SECURITY randomized clinical trial. *J Am Coll Cardiol* **64**, 2086, 2014.
- Mauri, L., Kereiakes, D.J., Yeh, R.W., *et al.* Twelve or 30 months of dual antiplatelet therapy after drug-eluting stents. *N Engl J Med* **371**, 2155, 2014.
- Duckers, H.J., Soullie, T., den Heijer, P., *et al.* Accelerated vascular repair following percutaneous coronary intervention by capture of endothelial progenitor cells promotes regression of neointimal growth at long term follow-up: final results of the Healing II trial using an endothelial progenitor cell capturing stent (Genous R stent). *Euro-Intervention* **3**, 350, 2007.
- Jantzen, A.E., Lane, W.O., Gage, S.M., *et al.* Use of autologous blood-derived endothelial progenitor cells at point-of-care to protect against implant thrombosis in a large animal model. *Biomaterials* **32**, 8356, 2011.
- Kempe, H., Kates, S.A., and Kempe, M. Nanomedicine's promising therapy: magnetic drug targeting. *Expert Rev Med Devices* **8**, 291, 2011.
- Pan, Y., Du, X., Zhao, F., and Xu, B. Magnetic nanoparticles for the manipulation of proteins and cells. *Chem Soc Rev* **41**, 2912, 2012.
- Chorny, M., Fishbein, I., Adamo, R.F., Forbes, S.P., Folchman-Wagner, Z., and Alferiev, I.S. Magnetically targeted delivery of therapeutic agents to injured blood vessels for prevention of in-stent restenosis. *Methodist Debaque Cardiovasc J* **8**, 23, 2012.

9. Chorny, M., Fishbein, I., Forbes, S., and Alferiev, I. Magnetic nanoparticles for targeted vascular delivery. *IUBMB Life* **63**, 613, 2011.
10. Pislaru, S.V., Harbuzariu, A., Gulati, R., *et al.* Magnetically targeted endothelial cell localization in stented vessels. *J Am Coll Cardiol* **48**, 1839, 2006.
11. Polyak, B., Fishbein, I., Chorny, M., *et al.* High field gradient targeting of magnetic nanoparticle-loaded endothelial cells to the surfaces of steel stents. *Proc Natl Acad Sci U S A* **105**, 698, 2008.
12. Pislaru, S.V., Harbuzariu, A., Agarwal, G., *et al.* Magnetic forces enable rapid endothelialization of synthetic vascular grafts. *Circulation* **114**, 1314, 2006.
13. Uthamaraj, S., Tefft, B.J., Klabusay, M., Hlinomaz, O., Sandhu, G.S., and Dragomir-Daescu, D. Design and validation of a novel ferromagnetic bare metal stent capable of capturing and retaining endothelial cells. *Ann Biomed Eng* **42**, 2416, 2014.
14. Uthamaraj, S., Tefft, B.J., Hlinomaz, O., Sandhu, G.S., and Dragomir-Daescu, D. Ferromagnetic bare metal stent for endothelial cell capture and retention. *J Vis Exp* **103**, e53100, 2015.
15. Tefft, B.J., Uthamaraj, S., Harburn, J.J., Klabusay, M., Dragomir-Daescu, D., and Sandhu, G.S. Cell labeling and targeting with superparamagnetic iron oxide nanoparticles. *J Vis Exp* **105**, e53099, 2015.
16. Moore, C.G., Carter, R.E., Nietert, P.J., and Stewart, P.W. Recommendations for planning pilot studies in clinical and translational research. *Clin Transl Sci* **4**, 332, 2011.
17. Gulati, R., Jevremovic, D., Peterson, T.E., *et al.* Diverse origin and function of cells with endothelial phenotype obtained from adult human blood. *Circ Res* **93**, 1023, 2003.
18. Lee, S.J., Jeong, J.R., Shin, S.C., *et al.* Nanoparticles of magnetic ferric oxides encapsulated with poly(D,L lactide-co-glycolide) and their applications to magnetic resonance imaging contrast agent. *J Magn Magn Mater* **272**, 2432, 2004.
19. Lee, S.J., Jeong, J.R., Shin, S.C., *et al.* Magnetic enhancement of iron oxide nanoparticles encapsulated with poly(D,L lactide-co-glycolide). *Colloid Surface A* **255**, 19, 2005.
20. Ge, G., Wu, H., Xiong, F., *et al.* The cytotoxicity evaluation of magnetic iron oxide nanoparticles on human aortic endothelial cells. *Nanoscale Res Lett* **8**, 215, 2013.
21. Yang, F.Y., Yu, M.X., Zhou, Q., Chen, W.L., Gao, P., and Huang, Z. Effects of iron oxide nanoparticle labeling on human endothelial cells. *Cell Transplant* **21**, 1805, 2012.
22. Yang, J.X., Tang, W.L., and Wang, X.X. Superparamagnetic iron oxide nanoparticles may affect endothelial progenitor cell migration ability and adhesion capacity. *Cytotherapy* **12**, 251, 2010.
23. Ingram, D.A., Mead, L.E., Tanaka, H., *et al.* Identification of a novel hierarchy of endothelial progenitor cells using human peripheral and umbilical cord blood. *Blood* **104**, 2752, 2004.
24. Lin, Y., Weisdorf, D.J., Solovey, A., and Hebbel, R.P. Origins of circulating endothelial cells and endothelial outgrowth from blood. *J Clin Invest* **105**, 71, 2000.
25. Chade, A.R., Zhu, X., Lavi, R., *et al.* Endothelial progenitor cells restore renal function in chronic experimental renovascular disease. *Circulation* **119**, 547, 2009.
26. Gulati, R., Jevremovic, D., Witt, T.A., *et al.* Modulation of the vascular response to injury by autologous blood-derived outgrowth endothelial cells. *Am J Physiol Heart Circ Physiol* **287**, H512, 2004.
27. Zohra, F.T., Medved, M., Lazareva, N., and Polyak, B. Functional behavior and gene expression of magnetic nanoparticle-loaded primary endothelial cells for targeting vascular stents. *Nanomedicine* **10**, 1391, 2015.
28. Danhier, F., Ansorena, E., Silva, J.M., Coco, R., Le Breton, A., and Preat, V. PLGA-based nanoparticles: an overview of biomedical applications. *J Control Release* **161**, 505, 2012.
29. Kumari, A., Yadav, S.K., and Yadav, S.C. Biodegradable polymeric nanoparticles based drug delivery systems. *Colloids Surf B Biointerfaces* **75**, 1, 2010.
30. Lo, C.T., Van Tassel, P.R., and Saltzman, W.M. Poly(lactide-co-glycolide) nanoparticle assembly for highly efficient delivery of potent therapeutic agents from medical devices. *Biomaterials* **31**, 3631, 2010.
31. Shive, M.S., and Anderson, J.M. Biodegradation and biocompatibility of PLA and PLGA microspheres. *Adv Drug Deliv Rev* **28**, 5, 1997.
32. Kwon, H.Y., Lee, J.Y., Choi, S.W., Jang, Y.S., and Kim, J.H. Preparation of PLGA nanoparticles containing estrogen by emulsification-diffusion method. *Colloid Surface A* **182**, 123, 2001.
33. Lemoine, D., Francois, C., Kedzierewicz, F., Preat, V., Hoffman, M., and Maincent, P. Stability study of nanoparticles of poly(epsilon-caprolactone), poly(D,L-lactide) and poly(D,L-lactide-co-glycolide). *Biomaterials* **17**, 2191, 1996.
34. Semete, B., Booyesen, L., Lemmer, Y., *et al.* In vivo evaluation of the biodistribution and safety of PLGA nanoparticles as drug delivery systems. *Nanomedicine* **6**, 662, 2010.
35. Corot, C., Robert, P., Idee, J.M., and Port, M. Recent advances in iron oxide nanocrystal technology for medical imaging. *Adv Drug Deliv Rev* **58**, 1471, 2006.
36. Provenzano, R., Schiller, B., Rao, M., Coyne, D., Brenner, L., and Pereira, B.J. Ferumoxytol as an intravenous iron replacement therapy in hemodialysis patients. *Clin J Am Soc Nephrol* **4**, 386, 2009.
37. Schwenk, M.H. Ferumoxytol: a new intravenous iron preparation for the treatment of iron deficiency anemia in patients with chronic kidney disease. *Pharmacotherapy* **30**, 70, 2010.
38. Levy, M., Luciani, N., Alloyeau, D., *et al.* Long term in vivo biotransformation of iron oxide nanoparticles. *Biomaterials* **32**, 3988, 2011.
39. Li, L., Jiang, W., Luo, K., *et al.* Superparamagnetic iron oxide nanoparticles as MRI contrast agents for non-invasive stem cell labeling and tracking. *Theranostics* **3**, 595, 2013.
40. Nkansah, M.K., Thakral, D., and Shapiro, E.M. Magnetic poly(lactide-co-glycolide) and cellulose particles for MRI-based cell tracking. *Magn Reson Med* **65**, 1776, 2011.
41. Granot, D., Nkansah, M.K., Bennewitz, M.F., Tang, K.S., Markakis, E.A., and Shapiro, E.M. Clinically viable magnetic poly(lactide-co-glycolide) particles for MRI-based cell tracking. *Magn Reson Med* **71**, 1238, 2014.
42. Yu, M., Huang, S., Yu, K.J., and Clyne, A.M. Dextran and polymer polyethylene glycol (PEG) coating reduce both 5 and 30 nm iron oxide nanoparticle cytotoxicity in 2D and 3D cell culture. *Int J Mol Sci* **13**, 5554, 2012.
43. Astanina, K., Simon, Y., Cavelius, C., Petry, S., Kraegeloh, A., and Kiemer, A.K. Superparamagnetic iron oxide nanoparticles impair endothelial integrity and inhibit nitric oxide production. *Acta Biomater* **10**, 4896, 2014.

44. Wu, X., Tan, Y., Mao, H., and Zhang, M. Toxic effects of iron oxide nanoparticles on human umbilical vein endothelial cells. *Int J Nanomedicine* **5**, 385, 2010.
45. Huang, Z.Y., Pei, N., Wang, Y.Y., *et al.* Deep magnetic capture of magnetically loaded cells for spatially targeted therapeutics. *Biomaterials* **31**, 2130, 2010.
46. Yellen, B.B., Forbes, Z.G., Halverson, D.S., *et al.* Targeted drug delivery to magnetic implants for therapeutic applications. *J Magn Magn Mater* **293**, 647, 2005.
47. Adamo, R.F., Fishbein, I., Zhang, K., *et al.* Magnetically enhanced cell delivery for accelerating recovery of the endothelium in injured arteries. *J Controlled Release* **222**, 169, 2016.
48. Polyak, B., Medved, M., Lazareva, N., *et al.* Magnetic nanoparticle-mediated targeting of cell therapy reduces in-stent stenosis in injured arteries. *ACS Nano* **10**, 9559, 2016.
49. Kempe, M., Kempe, H., Snowball, I., *et al.* The use of magnetite nanoparticles for implant-assisted magnetic drug targeting in thrombolytic therapy. *Biomaterials* **31**, 9499, 2010.
50. Chorny, M., Fishbein, I., Yellen, B.B., *et al.* Targeting stents with local delivery of paclitaxel-loaded magnetic nanoparticles using uniform fields. *Proc Natl Acad Sci U S A* **107**, 8346, 2010.
51. Rathel, T., Mannell, H., Pircher, J., Gleich, B., Pohl, U., and Krotz, F. Magnetic stents retain nanoparticle-bound antirestenotic drugs transported by lipid microbubbles. *Pharm Res* **29**, 1295, 2012.
52. Aviles, M.O., Chen, H.T., Ebner, A.D., Rosengart, A.J., Kaminski, M.D., and Ritter, J.A. In vitro study of ferromagnetic stents for implant assisted-magnetic drug targeting. *J Magn Magn Mater* **311**, 306, 2007.
53. Carter, A.J., Laird, J.R., Farb, A., Kufs, W., Wortham, D.C., and Virmani, R. Morphologic characteristics of lesion formation and time course of smooth muscle cell proliferation in a porcine proliferative restenosis model. *J Am Coll Cardiol* **24**, 1398, 1994.
54. Farb, A., Sangiorgi, G., Carter, A.J., *et al.* Pathology of acute and chronic coronary stenting in humans. *Circulation* **99**, 44, 1999.

Address correspondence to:
Gurpreet S. Sandhu, MD, PhD
Department of Cardiovascular Medicine
Mayo Clinic
200 First Street SW
Rochester, MN 55905

E-mail: sandhu.gurpreet@mayo.edu

Received: September 22, 2017

Accepted: January 25, 2018

Online Publication Date: March 12, 2018